EPJ Web of Conferences **303**, 05005 (2024) https://doi.org/10.1051/epjconf/202430305005
MENU 2023

Coordinate-space calculation of QED corrections to the hadronic vacuum polarization contribution to $(g-2)_\mu$ with SU(3) flavor symmetry

En-Hung Chao[4,], *Harvey B.* Meyer[1,2,3,], and *Julian* Parrino[1,*]

[1]PRISMA$^+$ Cluster of Excellence & Institut für Kernphysik,
Johannes Gutenberg-Universität Mainz, D-55099 Mainz, Germany
[2]Helmholtz Institut Mainz,
Staudingerweg 18, D-55128 Mainz, Germany
[3]GSI Helmholtzzentrum für Schwerionenforschung,
D-64291 Darmstadt, Germany
[4]Physics Department, Columbia University, New York, New York 10027, USA

Abstract. Lattice QCD (LQCD) has proven to be an important tool in understanding the tension between the experimental value for the anomalous magnetic moment of the muon $(g-2)_\mu$ and its prediction from the standard model. The lattice provides a non-perturbative method for evaluating the hadronic contributions to $(g-2)_\mu$, which contributes the largest amount to the uncertainty of the theoretical prediction. Among these the hadronic vacuum polarization a_μ^{HVP} is the dominant contribution. In order to match the uncertainty of the experiment, lattice QCD needs to reach sub-percent precision. This requires the calculation of QED corrections to a_μ^{HVP}, which are represented by additional Feynman diagrams. We present a lattice calculation of the UV-finite $(2+2)$ diagram at the SU(3) flavor symmetric point and compare this to the pseudoscalar meson exchange model with a vector-meson dominance parametrization of the transition form factor.

1 Introduction

The Standard Model prediction for the anomalous magnetic moment of the muon $(g-2)_\mu$ being in tension with the experimental result has been an unsolved problem for many years now. With great effort on improving the accuracy of the experiment, a precision of 0.20 ppm [1] has been reached. From the viewpoint of the theory also a lot has been accomplished. The QED contributions to $(g-2)_\mu$, which make up the largest contribution are known to 0.9 ppb. However, the largest part of the uncertainty of the theory result stems from hadronic contributions. Here, the leading order hadronic vacuum polarization a_μ^{HVP}, entering at $O(\alpha^2)$ in the fine structure constant α, is the dominant one.

The determination of a_μ^{HVP} from lattice QCD has driven some new innovations to reach for higher precision. Among these methods is the covariant coordinate-space method (CCS), first proposed in Ref. [2]. This representation does not rely on the choice of a specific momentum frame as the time-momentum representation (TMR) [3] does, traditionally used for

*e-mail: juparrin@uni-mainz.de

Id	β	$L^3 \times T$	a [fm]	m_π [MeV]	m_K [MeV]	$m_\pi L$	L [fm]	#confs light
N202	3.55	$48^3 \times 128$	0.06426	410(5)	410(5)	6.4	3.1	200

Table 1: The parameters of the ensemble N202 generated by the CLS consortium. The lattice spacing is determined in Ref. [9] and the pion and kaon mass are taken from Ref. [10].

the calculation of a_μ^{HVP}. Additionally the CCS method offers flexibility in choosing a suitable integral kernel to adjust the integrand.

In Ref. [4], a complete calculation of a_μ^{HVP} at an unphysical pion mass of $\sim$ 350 MeV was carried out thus giving a blueprint for a calculation in the CCS representation, including the treatement of finite-volume effects. To match the experimental precision it is necessary to include QED corrections in the form of additional Fenyman diagrams at $O(\alpha^3)$. In Ref [5] we proposed a framework for these corrections using an extension of the CCS method, similar to the calculation of the hadronic light-by-light contribution [6, 7], using a Pauli-Villars regularization of the photon propagator to address the UV-divergence of a_μ^{HVP} at next-to-leading order (NLO). In Ref. [8] we have obtained first results for the intrinsically-UV-finite contribution of the $(2+2)$ topology. These results have been in good agreement with the prediction of the pseudoscalar meson exchange contribution. In these proceedings we want to complement this calculation with one additional lattice ensemble at the SU(3) flavor symmetric point, where the up, down and strange quark are mass degenerate.

2 Coordinate-space method for the HVP at next-to-leading order

We use the covariant coordinate-space (CCS) representation for the hadronic vacuum polarizaton contribution a_μ^{HVP}, first derived in [2].

$$a_\mu^{HVP} = \int_z H_{\mu\sigma}(z)\langle j_\mu(z) j_\sigma(0)\rangle, \tag{1}$$

with the CCS kernel $H_{\mu\sigma}(z) = -\delta_{\mu\sigma}\mathcal{H}_1(|z|)+\frac{z_\mu z_\sigma}{|z|^2}\mathcal{H}_2(|z|)$ and the electromagnetic vector current $j_\mu(z) = \frac{2}{3}\bar{u}(z)\gamma_\mu u(z) - \frac{1}{3}\bar{d}(z)\gamma_\mu d(z) - \frac{1}{3}\bar{s}(z)\gamma_\mu s(z) + \ldots$. It is also possible to obtain the HVP contribution to the vacuum polarization $\Pi(Q^2)$ by replacing the functions $\mathcal{H}_1$ and $\mathcal{H}_2$ with the appropriate ones, given in Ref. [2]. Expanding the vector-vector correlator $\langle j_\mu(z) j_\sigma(0)\rangle$ in the electromagnetic coupling $e = \sqrt{4\pi\alpha}$ we obtain

$$\langle j_\mu(z) j_\sigma(0)\rangle = \langle j_\mu(z) j_\sigma(0)\rangle_{QCD} - \frac{e^2}{2}\int_{x,y}\delta_{\nu\rho}\Big[G_0(y-x)\Big]_\Lambda \langle j_\mu(z) j_\nu(y) j_\rho(x) j_\sigma(0)\rangle_{QCD} + \text{counterterms} + O(e^4), \tag{2}$$

where now only the QCD vacuum expectation value $\langle\ldots\rangle_{QCD}$ needs to be evaluated with respect to gluon interactions between all valence quarks. To regulate the divergence that arises when $x \to y$ in the argument of the photon propagator $G_0(x-y)$, we introduce a Pauli-Villars regulator, first proposed in Ref. [5]

$$\Big[G_0(y-x)\Big]_\Lambda = \frac{1}{4\pi^2|y-x|^2} - \frac{\Lambda K_1(\Lambda|y-x|)}{4\pi^2|y-x|}, \tag{3}$$

where $K_1(x)$ is the modified modified Bessel function of the second kind. Thus, we define the next-to-leading order QED corrections to a_μ^{HVP} as

$$a_\mu^{HVP,NLO} = -\frac{e^2}{2}\int_{x,y,z} H_{\mu\sigma}(z)\delta_{\nu\rho}\Big[G_0(y-x)\Big]_\Lambda \langle j_\mu(z) j_\nu(y) j_\rho(x) j_\sigma(0)\rangle_{QCD} \tag{4}$$

We use the expressions for the $H_{\mu\sigma}(z)$ and $\Big[G_0(y-x)\Big]_\Lambda$ in the continuum. Only the four-point function $\langle j_\mu(z) j_\nu(y) j_\rho(x) j_\sigma(0)\rangle_{QCD}$ is evaluated on the lattice in isospin symmetric QCD. After including the necessary counterterms, the dependence on Λ can be scrutinized for the onset of a plateau, while keeping $a\Lambda \ll 1$. Alternatively, one can add a further $O(e^2)$ correction computed with a lattice-regularized photon propagator of mass Λ [5], thereby raising the maximum photon virtuality to the lattice cutoff scale.

One needs to include all possible Wick-contractions contributing to $\langle j_\mu(z) j_\nu(y) j_\rho(x) j_\sigma(0)\rangle_{QCD}$. These can be labeled by the number of vector currents that are connected by valence quark lines, as depicted in Ref. [8]. At the SU(3) flavor symmetric point, where up, down and strange quark are mass degenerate, all diagrams that contain a self-contracted vector current, e.g. $(3+1)$, $(2+1+1)$, $(1+1+1+1)$ cancel out, because the light and strange quark contributions to the self-contracted loops cancel out exactly in this case.

In the following we will concentrate on the $(2+2)a$ contribution, defined in Ref. [8] as the diagram in which the photon connects two different quark loops. Since this contribution is UV-finite, we drop the Pauli-Villars regulator. We compute and store in position space the quark loop containing two electromagnetic vertices. The calculation is performed on one ensemble, see Table 1. The simulation is performed with $N_f = 2+1$ dynamical flavors of non-perturbatively $O(a)$ improved Wilson quarks and tree-level $O(a^2)$ improved Lüscher-Weisz gauge action. For these two-point functions we use 24 different point-sources distributed along the spatial diagonal $(2n, 2n, 2n, 64)$ for $n = \{0, 1, \ldots, 23\}$. At the SU(3) symmetric point the relevant charge factor for the $(2+2)$ contributions is given by $\frac{36}{81}$ accounting for all possible contractions of up, down and strange quarks.

3 Pseudoscalar meson exchange at the SU(3) symmetric point

Analogous to the the hadronic light-by-light scattering [11], we expect the dominant part of the $(2+2)$ contributions to be explained by the pseudoscalar meson exchange (PME). We calculate the total PME contribution using Eq. (12) of Ref. [8], where we use the result from Ref. [12] for the momentum-space four-point function. We use the vector-meson dominance (VMD) parametrization of the transition formfactor. The total PME contribution is then parametrized by the mass of the meson m, the VMD mass m_V and the normalization of the transition formfactor $\mathcal{F}(0,0) = (4\pi^2 f)^{-1}$. We include contributions from the π^0, η and η'. Having computed their total contribution to $a_\mu^{HVP,NLO}$, one needs to determine to what extent the individual pseudoscalar mesons contribute to the $(2+2)a$ diagram. The $(2+2)$ contributions in QCD matches to the t-channel contributions in the PME model [6]. For the $(2+2)b$ diagram, in which the internal photon belongs to one of the quark loops, the PME vanishes.

At the SU(3) symmetric point, it is straightforward to obtain the necessary weight factors for the π^0, η and η', see Ref. [11]. With the π^0 and η being a part of the octet, both are mass degenerate and contribute with a factor of -2 relative to the total $a_\mu^{HVP,NLO}$ contribution. In contrast, the fully-connected diagram receives contributions from the PME with a weight factor of 3, which corrects for the deficiency and leads to the correct fully PME contribution upon considering the complete set of diagrams. The singlet η' contributes with weight 1 to

	$a_\mu \cdot 10^{12}$	$[\tilde{\Pi}(1GeV^2, 0.25GeV^2)] \cdot 10^7$
H^{TL}	-50(16)	-51(16)
H^{XX}	-49(15)	-55(17)
π^0	-39	-80
η	-13	-27
η'	24	57
$\pi^0 + \eta + \eta'$	-27(4)	-49(8)

Table 2: Results for the integrated quantity. The results for the PME are integrated up to infinity. The lattice results for the subtracted vacuum polarization $\tilde{\Pi}(1GeV^2, 0.25GeV^2)$ are integrated up to $|x| \sim 2$ fm.

the (2 + 2) diagrams and does not contribute to the fully-connected diagrams. Furthermore we know that the coupling of the η to two photons is exactly $\frac{1}{\sqrt{3}}$ of that of the π^0 at the SU(3) symmetric point, therefore the η contribution to $a_\mu^{HVP,NLO}$ is $\frac{1}{3}$ of the π^0 contribution [11]. The complete parameters of our model are $(m_\pi, m_{V,\pi}, f_\pi)$ and $(m_{\eta'}, m_{V,\eta'}, f_{\eta'})$. The pion mass m_π and decay constant f_π are taken from Ref. [10]. The rho-meson mass is obtained from fitting the single-virtual data from Ref. [13] to a VMD-parametrized pion transition form factor [11]. We use the same parameters for $m_{V,\eta}$ and f_η as in Ref. [6], but we take the mass m_η from Ref. [14] computed on the same lattice ensemble. In total we have $(m_\pi, m_{V,\pi}, f_\pi) = (412, 952, 110)$ MeV and $(m_{\eta'}, m_{V,\eta'}, f_{\eta'}) = (1016, 952, 74)$ MeV.

4 Results

We integrate over y and z and the angular part of x in Eq.4 and display the remaining |x|-integrand in Fig. 1 for (a) the contribution to $a_\mu^{HVP,NLO}$ and (b) the subtracted vacuum polarization $\tilde{\Pi}(1GeV^2, 0.25GeV^2) := \Pi(1GeV^2) - \Pi(0.25GeV^2)$. The results of the integrated values are given in Table 2. We see that for the case of $\tilde{\Pi}(1GeV^2, 0.25GeV^2)$ the model prediction fits very well to the lattice data for both kernels. This is especially remarkable because there is a large cancellation happening between the π^0 and η and the η' contribution and all parameters of the PME are taken from separate evaluations. For the case of the contribution to $a_\mu^{HVP,NLO}$ the model describes the data up to ~ 0.8 fm but deviates for larger $|x|$. The kernel for a_μ is much more long-ranged than the kernel for $\tilde{\Pi}(1GeV^2, 0.25GeV^2)$, therefore the contribution to a_μ is more sensible to noise in the correlator at large $|x|$. This can be seen from the fact that the errorbars are larger in Fig. 1a.

5 Conclusion

We studied the behaviour of the (2 + 2)a diagram. At the SU(3) flavor symmetric point the total number of model parameters is reduced due to the η being degenerate with the π^0. There is also no ambiguity for the weight factors, since in our model there is no mixing between η and η' at this point. Our findings are in in good agreement with the results of Ref. [8]: The PME gives a reasonable good description for the (2 + 2)a diagram, especially for the case of the subtracted vacuum polarization. However, it would be very interesting to examine the pion mass dependence of the (2 + 2)a contribution up to the physical point, to see how the mixing of η and η' as well as the charged pion loop affects the modeling of the integrand via the PME.

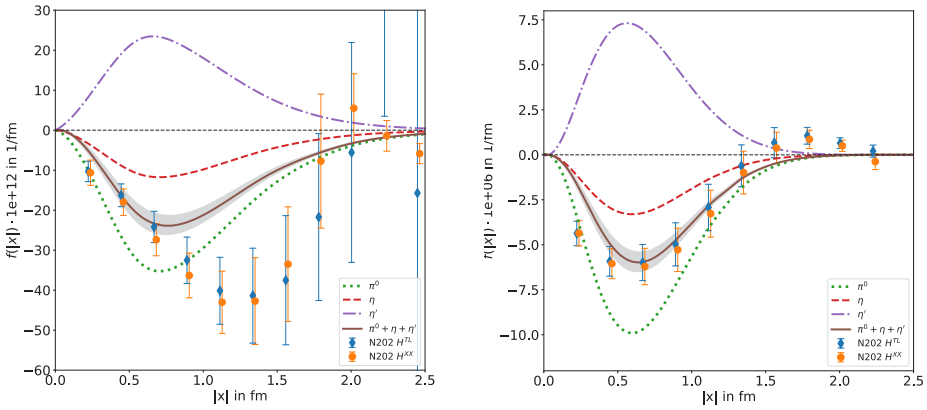

(a) (2+2)a contribution to $a_\mu^{HVP,NLO}$

(b) (2+2)a contribution to $\tilde{\Pi}(1GeV^2, 0.25GeV^2)$

Figure 1: Comparison between the lattice data on one ensemble (N202) for the 'TL' and 'XX' kernel, defined in Ref. [8], and the pseudoscalar exchange model. The 'XX' kernel is slightly displaced for better readability.

References

[1] D.P. Aguillard et al. (Muon g-2) (2023), 2308.06230
[2] H.B. Meyer, Eur. Phys. J. C **77**, 616 (2017), 1706.01139
[3] D. Bernecker, H.B. Meyer, Eur.Phys.J. **A47**, 148 (2011), 1107.4388
[4] E.H. Chao, R.J. Hudspith, A. Gérardin, J.R. Green, H.B. Meyer, Eur. Phys. J. C **82**, 664 (2022), 2204.08844
[5] V. Biloshytskyi, E.H. Chao, A. Gérardin, J.R. Green, F. Hagelstein, H.B. Meyer, J. Parrino, V. Pascalutsa, JHEP **03**, 194 (2023), 2209.02149
[6] E.H. Chao, R.J. Hudspith, A. Gérardin, J.R. Green, H.B. Meyer, K. Ottnad, Eur. Phys. J. C **81**, 651 (2021), 2104.02632
[7] T. Blum, N. Christ, M. Hayakawa, T. Izubuchi, L. Jin, C. Jung, C. Lehner, C. Tu (2023), 2304.04423
[8] E.H. Chao, H.B. Meyer, J. Parrino, *Coordinate-space calculation of QED corrections to the hadronic vacuum polarization contribution to* $(g-2)_\mu$, in *40th International Symposium on Lattice Field Theory* (2023), 2310.20556
[9] M. Bruno, T. Korzec, S. Schaefer, Phys. Rev. D **95**, 074504 (2017), 1608.08900
[10] M. Cè et al., Phys. Rev. D **106**, 114502 (2022), 2206.06582
[11] E.H. Chao, A. Gérardin, J.R. Green, R.J. Hudspith, H.B. Meyer, Eur. Phys. J. C **80**, 869 (2020), 2006.16224
[12] M. Knecht, A. Nyffeler, Phys. Rev. D **65**, 073034 (2002), hep-ph/0111058
[13] A. Gérardin, M. Cè, G. von Hippel, B. Hörz, H.B. Meyer, D. Mohler, K. Ottnad, J. Wilhelm, H. Wittig, Phys. Rev. **D100**, 014510 (2019), 1904.03120
[14] G.S. Bali, V. Braun, S. Collins, A. Schäfer, J. Simeth (RQCD), JHEP **08**, 137 (2021), 2106.05398